

## New Insight into the SAR of Pyrimido [4,5-b][1,4] Benzothiazines as 15-lipoxygenase Inhibitors

Nona Pooryaghoobi<sup>1</sup>, Mehdi Bakavoli<sup>2</sup>, Maliheh Alimardani<sup>3</sup>, Tahmineh Bazzazan<sup>2</sup>, Hamid Sadeghian<sup>4,5\*</sup>

<sup>1</sup>Department of Chemistry, Mashhad Branch, Islamic Azad University, Mashhad, IR Iran

<sup>2</sup>Department of Chemistry, School of Sciences, Ferdowsi University of Mashhad, Mashhad, 917751436, IR Iran

<sup>3</sup>Student Research Committee, Department of Laboratory Sciences, School of Paramedical Sciences, Mashhad University of Medical Sciences, Mashhad, IR Iran

<sup>4</sup>Antimicrobial Resistance Research Center, Mashhad University of Medical Sciences, Mashhad 91967-73117, IR Iran

<sup>5</sup> Department of Laboratory Sciences, School of Paramedical Sciences, Mashhad University of Medical Sciences, Mashhad, IR Iran

### ARTICLE INFO

#### Article type:

Original article

#### Article history:

Received: May 30, 2012

Accepted: Oct 10, 2012

#### Keywords:

DMAB

Docking

MBTH

Peroxide formation

SLO

### ABSTRACT

**Objective(s):** Recently we reported that the soybean 15-lipoxygenase (SLO) inhibitory activity of pyrimido[4,5-b][1,4]benzothiazines largely depends on the orientation of sulfur atom of thiazine core towards Fe<sup>III</sup>-OH in the active site pocket of the enzyme with subsequent oxidation of sulfur to sulfoxide. In this paper the results of a comparative study on the SLO inhibitory activities of the mentioned compounds using *ab initio* calculations and docking analyses has been reported.

**Materials and Methods:** Structure optimization and docking analyses were performed using HyperChem 7.5 and AutoDock Tools 4.0 respectively. Enzyme assessment was reduced using spectrophotometric MBTH-DMAB method.

**Results:** The inhibitory activity of synthetic 2-substituted pyrimido[4,5-b][1,4]benzothiazines against soybean 15-lipoxygenase (SLO) was evaluated and structure activity relationships and binding modes of their 4-H and 4-methyl analogs were studied using docking analysis and *ab initio* calculations.

**Discussion:** The results of these studies showed that the lack of 4-methyl substituent in the pyrimido[4,5-b][1,4]benzothiazine molecules greatly reduces their lipoxygenase inhibitory activities and it was also found that the HOMO energy difference between the 4-H and 4-Methyl analogs can be responsible for the observed inhibitory activity reduction.

**Conclusion:** Our molecular modeling studies shows that by using more flexible amino acids during the docking process, more rational results can be obtained. The method of measuring the lipoxygenase activity is also of prime importance for the study of structure activity relationship.

#### ► Please cite this paper as:

Pooryaghoobi N, Bakavoli M, Alimardani M, Bazzazan T, Sadeghian H. New Insight into the SAR of Pyrimido [4,5-b][1,4] Benzothiazines as 15-lipoxygenase Inhibitors. Iran J Basic Med Sci; 2013; 16: 784-789.

### Introduction

It is well documented that mammalian lipoxygenases (LO's) are non-heme iron-containing enzymes responsible for the oxidation of polyunsaturated fatty acids and esters to hydroperoxy derivatives (1). These are heterogeneous families of enzymes distributed widely throughout the plant and animal kingdoms (2), and named according to the position at which a key substrate, arachidonic acid (AA), is oxidized. Among the mammalian lipoxygenases involved in the etiology of human disease, 5-lipoxygenase (5-LO) is now well established as a target for reducing the production of leukotrienes (important in particular asthma) (3, 4). More recently, 15-lipoxygenase (15-LO) has emerged as an attractive target for

therapeutic intervention (5). 15-LO has been implicated in the progression of certain cancers (6, 7) and chronic obstructive pulmonary disease (COPD) (6).

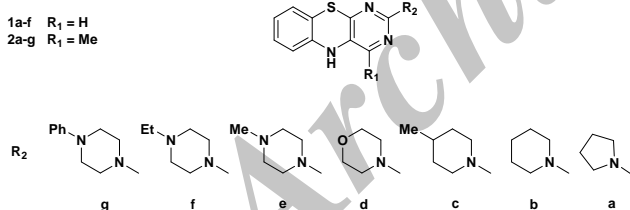
Evidence for the inhibition of 15-LO in the treatment of vascular disease is, however, most compelling (8). Both transgenic and knockout studies implicate a role for 15-LO in atherogenesis (9,10). The enzyme is abundantly expressed in macrophages residing within the atherosclerotic lesion (10). In addition, the immediate products of 15-LO oxidation of AA and linoleic acid (LA) have been shown to be pro-inflammatory (11) and pro-thrombotic (12).

\*Corresponding author: Hamid Sadeghian, Antimicrobial Resistance Research Center, Mashhad University of Medical Sciences, Mashhad 91967-73117, Iran, Tel.: +9805117112611, Fax: +9805117112596; email: sadeghianh@mums.ac.ir

It is also found that 15-LO is linked to cardiovascular complications since it is known to participate in oxidative modification of low-density lipoproteins (LDL) leading to the development of atherosclerosis (13).

Three different strategies have been developed to inhibit the LO's pathway (12). They involve (i) redox inhibitors or antioxidants, which interfere with the redox cycle of 15-LO, (ii) iron-chelator agents, and (iii) non-redox competitive inhibitors, which compete with AA to bind the enzyme active site.

Recently we reported the results of our studies on the soybean 15-lipoxygenase (SLO) inhibitory activities of some pyrimido[4,5-b][1,4]benzothiazines derivatives **1a-f** and **2a-f** and on the basis of the structure activity relationship (SAR) studies we suggested that the inhibitory activity of these molecules largely depends on the orientation of sulfur atom of thiazine core towards chelated Fe<sup>III</sup>-OH in the active site pocket of the enzyme with subsequent oxidation of sulfur to sulfoxide (14, 15). In this paper we wish to report the results of a comparative study on the SLO inhibitory activities of a group of pyrimido[4,5-b][1,4]benzothiazines and their 4-H and 4-methyl analogs (Scheme 1) using *ab initio* calculations and docking analysis. In the research other lipoxygenase inhibitory assessment in which the enzyme activity measurement was made is also used according to the reported peroxide formation protocols (16). In the other work the three dimensional structural requirements of some natural organosulfur compounds for SLO inhibitory activity using comparative molecular field analysis (CoMFA) and comparative molecular similarity indices analysis (CoMSIA) was studied (17).



**Scheme 1:** chemical structure of compounds 1a-f and 2a-f

## Materials and Methods

### Chemistry

Compounds **1a-f** and **2a-f** were synthesized according to the procedure reported in the previous literatures by starting from uracil and 4-methyluracil as primary reagents (14, 15).

### Structure optimization

Structures **1a-f** and **2a-f** were simulated in chem3D professional; Cambridge software (18); using MM2 method (RMS gradient = 0.1 kcal mol<sup>-1</sup>) (19, 20). In the second optimization, output files were minimized under Semiempirical AM1 methods

(Convergence limit = 0.01; Iteration limit=50; RMS gradient = 0.1 kcal mol<sup>-1</sup>; Polak-Ribiere optimizer algorithm) then the output files were minimized under *ab initio* methods with 6-311G\* basis set (Convergence limit=1e-5; Iteration limit=50; RMS gradient=0.1 kcal mol<sup>-1</sup>; Polak-Ribiere optimizer algorithm Hyper Chem7.5 (21). After geometry optimization and docking, single point properties of docked molecules such as energy of HOMO and LUMO were calculated using *ab initio* method with 6-311G\* basis set (convergence limit= 1e-5; iteration limit= 50). The initial guess of the MO coefficients is from eigenvectors of the core Hamiltonian in HyperChem 7.5 (21).

Crystal structure of soybean lipoxygenase-3 (arachidonic acid 15-lipoxygenase) complex with 13(S)-hydroproxy-9 (Z)-2,11(E)-octadecadienoic acid was retrieved from RCSB Protein Data Bank (PDB entry: 1IK3).

### Molecular docking

Automated docking simulation was implemented to dock **1a-f** and **2a-f** into the active site of SLO with Auto Dock Tools version 4.2 (revision 30) (22) using Lamarckian genetic algorithm (23). This method has been previously shown to produce bonding models similar to the experimentally observed models (16, 24, 25). The torsion angles of the ligands were identified, hydrogens were added to the macromolecule, bond distances were edited and solvent parameters were added to the enzyme 3D structure. Partial atomic charges were then assigned to the macromolecule as well as ligands (Gasteiger for the ligands and Kollman for the protein) (26).

The regions of interest of the enzyme were defined by considering Cartesian chart 20.5, 3.5 and 20.45 as the central of a grid size of 42, 42 and 56 points in X, Y and Z axes. Ile557, Ile566, Ile572, Ile515, Phe576, Leu770 and Ile773 were selected flexible. The docking parameter files were generated using Genetic Algorithm and Local Search Parameters (GALS) while number of generations was set to 256. The 256 docked complexes were clustered with a root-mean-square deviation tolerance of 0.2 Å. The program generated 256 compound **1a-f** and **2a-f** docked conformers corresponding to the lowest-energy structures. After docking procedure, docking results were submitted to DS visualize (27) for further evaluations.

### SLO screening assay

Linoleic acid and two assay solutions (A and B) were prepared in advance. Solution A was 50 mM DMAB in a 100 mM phosphate buffer (pH 7.0). Solution B was a mixture of 10 mM MBTH (3 mL), hemoglobin (5 mg/mL, 3 mL) in 50 mM phosphate buffer at pH 5.0 (25 mL). A linoleic acid solution was prepared by mixing 5 mg of linoleic acid with 0.5 mL ethanol and then diluting with KOH 100 mM to a final volume of 5 mL. In the standard assay, the

sample in ethanol (25  $\mu$ L), SLO (4000 units/mL in 50 mM phosphate buffer pH 7.0; 25  $\mu$ L) and phosphate buffer pH 7.0 (50 mM; 900  $\mu$ L) were mixed in a test tube and preincubation was carried out for 5 min at room temperature. A control test was done with the same volume of ethanol. After the pre-incubation, linoleic acid solution (50  $\mu$ L) was added to start the peroxidation reaction, and, 7 min later, solution A (270  $\mu$ L) and then solution B (130  $\mu$ L) was added to start the color formation. 5 min later, 200  $\mu$ L of a 2% SDS solution was added to terminate the reaction. The absorbance at 598 nm was compared with control test. The  $IC_{50}$  results are outlined in Table 1.

## Results

Structural optimization of the more stable conformers of the mentioned pyrimidobenzothiazines, revealed that for each structure two enantiomers are prone to exist (Figure 1). It can be argued that the presence of these configurations arises from slight bending in the plane of the thiazine ring. In these structures the bond angle between sulfur and two of its adjacent carbon atoms are out-of-plane, bending downwards, which ultimately produces an unsymmetrical structure. It is well documented that the lower the tendency of sulfur pi orbital to participate in  $sp^3$  hybridization, the more the bending; and because of its electron donating and reducing properties inhibitory role of the sulfur atom increases in thiazine ring. It has also been proved that in the process of the enzyme inhibition, the sulfur atom undergoes oxidation (14).

The optimized three dimensional structures of compounds **1a-f** and **2a-f** were docked into the active site of the SLO using Auto dock Tools software. The side chain of the hydrophobic amino acids Ile515, Ile557, Leu565, Ile566, Ile572, Phe576, Leu770 and Ile773 which have had direct contact to the substrate in the active site pocket of the enzyme were considered to be flexible. In the docking process, for every compound 256 docked models were obtained among them 25 to 45 percent belongs to a cluster with the sulfur atom oriented vertically towards the Iron atom which is attached to the enzyme. In the software the estimated free bonding energy ( $\Delta G_b$ ) and inhibitory constant ( $K_i$ ) of each docked model was calculated and outputted as Kcal/mol and mol/L respectively (Table 1). Among the two enantiomers of compound, the ones with the plane of pyrimidobenzothiazine bending downwards and the sulfur atom in-front with the amine substituent on the right side of the molecule (Figure 1: right) were the responsible



**Figure 1.** Two enantiomers of compound 2e derived from structural optimization

models for forming the aforementioned conformation in the active site pocket. The thiazine ring was fixed with two amino acids Leu565, Leu773 and the substituents of the pyrimidine ring were surrounded by the pocket of the amino acids Leu770, Val769, Asp766, Gln716, Phe576, Ile572 and Gln514 (Figure 2).

It is interesting to note that the aforementioned amino acids with the exception of Val769 and Phe576 are conserved (18, 19). In the selected cluster for every docked substituent, the model with the least inhibitory constant ( $K_i$ ) was chosen as "consensus structure" to study its structure-activity relationship (Figure 2). The inhibitory activity of compounds **1a-f**, **2a-f** towards SLO enzyme was determined by measuring the amount of peroxide formation. In this method, with the help of a spectrophotometer and by using a mixture of MBTH (3-methyl-2-benzothiazolonhydrazone) and DMAB (3-dimethylaminobenzoic acid) indicators in the presence of hemoglobin at the wavelength of 598 nm, the peroxide concentration was determined (16).

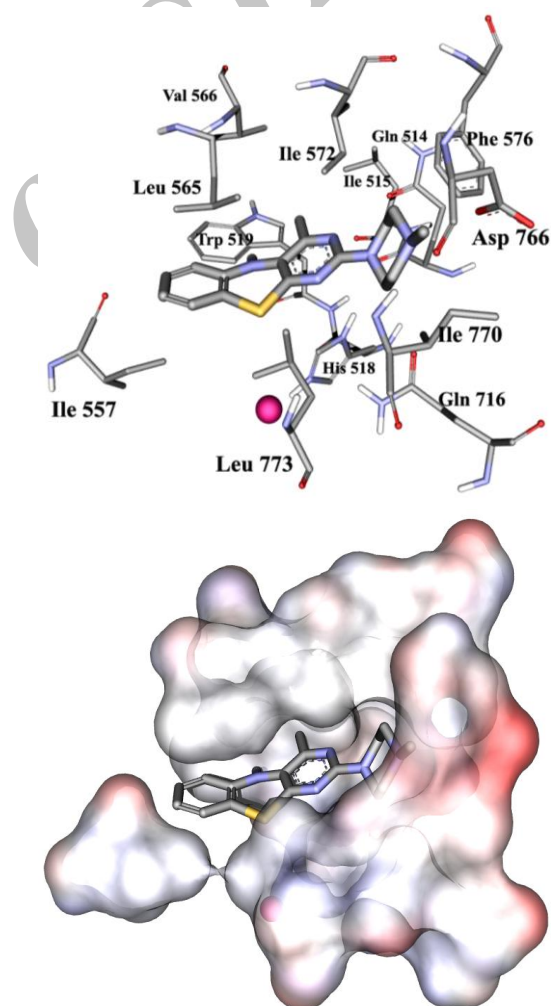


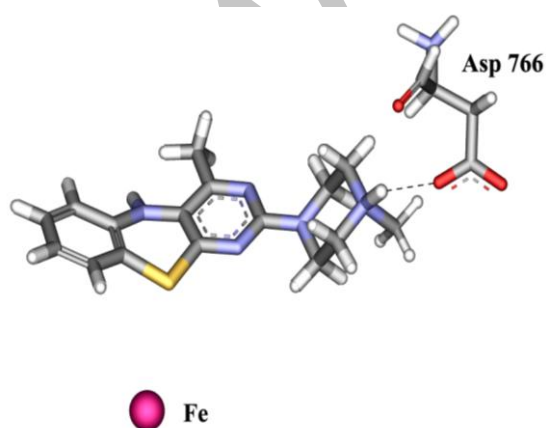
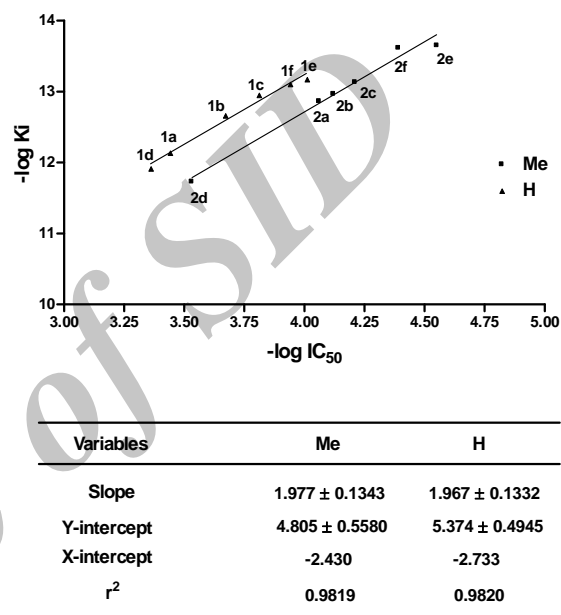
**Figure 2.** Consensus structure of 2e in the active site pocket of SLO in stick (above) and solvent surface (below) views. Fe atom is distinguished by pink ball. Carbon, oxygen, nitrogen, sulfur and hydrogen atoms are distinguished by gray, red, blue, yellow and white color respectively

**Table 1.** Docking processing data, enzyme inhibitory assessment and  $E_{\text{HOMO}}$  and  $E_{\text{LUMO}}$  of consensus structures (the  $\text{IC}_{50}$  values are given as mean  $\pm$  SD)

Compound	$\Delta G_b$	$K_i$ (fM)	$\text{IC}_{50}$ ( $\mu\text{M}$ )	$E_{\text{HOMO}}$ (ev)	$E_{\text{LUMO}}$ (ev)
1a	-16.56	726	$363.1 \pm 8.1$	-7.053	2.761
1b	-17.28	215.62	$203.8 \pm 6.4$	-7.384	2.689
1c	-17.67	110.85	$154.9 \pm 3.1$	-7.432	2.625
1d	-16.26	1210	$536.5 \pm 8.8$	-7.366	2.612
1e	-17.97	66.82	$87.7 \pm 2.1$	-7.024	2.762
1f	-17.88	77.66	$124.8 \pm 2.8$	-7.125	2.763
2a	-17.55	135.73	$197.1 \pm 2.4$	-7.143	2.825
2b	-17.70	109.94	$125 \pm 2.1$	-7.373	2.742
2c	-17.92	72.97	$107.6 \pm 2.1$	-7.127	2.799
2d	-16.01	1840	$395.1 \pm 5.1$	-7.194	2.639
2e	-18.49	28.04	$21.2 \pm 1.1$	-7.067	2.790
2f	-18.58	24.04	$40.7 \pm 1.3$	-7.009	2.793

## Discussion

Considering the data of Table 1 we can see among the two series of the synthetic compounds the lowest  $\text{IC}_{50}$  and  $K_i$  belong to **1e** and **2e** which have had the N-methyl piperazine moiety. This might be due to the hydrogen bonding formation between protonated tertiary terminal amine and carboxylate portion of conserved Asp766. To prove the hypothesis the inhibitory activity of **1e** and **2e** in comparison with **1c** and **2c** was performed at higher pH (pH = 8.3 versus pH = 7.0). The results showed that the  $\text{IC}_{50}$  of **1e** and **2e** increase to 129.2 and 39.2  $\mu\text{M}$  while it was nearly unchanged for **1c** and **2c** which have had methyl piperidine moiety. This behavior originated from protonation decrease of N-methyl piperazine moieties at higher pH. Also it is seen that by changing N-methyl piperazine to N-ethyl piperazine (increase of steric hindrance) the  $\text{IC}_{50}$  value increases. For further proof, the bulkier analog **2g** with N-phenyl piperazine moiety and lower protonation potency was tested for SLO inhibitory activity. The  $\text{IC}_{50}$  value of **2g** was 182  $\mu\text{M}$  which could be another witness for the protonation assertion.

**Figure 3.** 3D view of hydrogen bond between protonated N-methyl piperazine moiety of compound **2e** and carboxylate moiety of Asp766**Figure 4.** Diagram of  $(-\log K_i)$  versus  $(-\log \text{IC}_{50})$  for compounds 1a-f and 2a-f and the relevant data obtained from this diagram. The data of 4-methyl and 4-H pyrimidobenzothiazine analogs are distinguished by Me and H

Finally, the linear dependence of the inhibitory constants ( $K_i$ ) of the consensus structures versus the results obtained from the enzyme assay ( $\text{IC}_{50}$ ) was studied and is plotted graphically (Figure 4). As it can be seen in Figure 4 linear plots are obtained with the same gradient but different Y-intercept. This diagram shows that by using molecular simulating software such as Auto dock Tools for pyrimidobenzothiazines, we can predict the inhibitory activity of these substituents by changing the substitution at position 2 providing that the size of the substituents does not change dramatically. On the other hand, these plots clearly show the importance of the methyl substituent at position 4. As can be seen, by putting a methyl substituent at this position, the inhibitory activity increases dramatically which indicate the inhibitory potential of position 4 of the pyrimidobenzothiazines. Previously we showed that the methyl group can fill the hydrophobic cavity formed by Leu515, Trp519,

Val566 and Ile572 side chains and it might be one of the reasons of increase in inhibitory activity (15).

In a parallel investigation, the fluctuation in the energy state of HOMO was calculated using single point calculations for a hypothetical reaction concerning the transformation of the consensus structure 4-Me to 4-H, which was followed by using the following relation to obtain the equilibrium constant (K) for the hypothetical process:

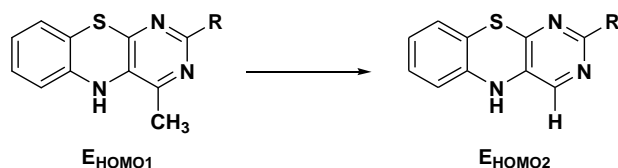
$$\Delta G^\circ = \Delta H^\circ - T\Delta S^\circ$$

$$\Delta S^\circ \sim 0 \Rightarrow \Delta G^\circ = \Delta H^\circ \Rightarrow \Delta G^\circ =$$

$$\Delta E_{\text{HOMO}} = -2.3RT \log K$$

$$\log K = -\Delta E_{\text{HOMO}} / 2.3RT$$

$$\Delta E_{\text{HOMO}} = E_{\text{HOMO}2} - E_{\text{HOMO}1}$$



It is interesting that the average of the aforementioned calculated K ( $K = 0.655$ ) is closed to Y-intercept difference ( $5.374 - 4.805 = 0.5690$ ) of the diagram in Figure 4.

By adding the average equilibrium constants to the Y-intercept of new 4-Me analogs, the following new linear plot was obtained. It seems that by changing the substituents at position 2, different analogs of 4-H and 4-Me will be obtained whose their inhibitory activity can be predicted by obtaining their  $K_i$  using Auto dock Tools and calculating their  $IC_{50}$  from the following equation:

$$\log K_i = (2.081 \pm 0.0803) \log IC_{50} - (4.334 \pm 0.3163)$$

The results of our investigations regarding the previously mentioned derivatives show that any changes in HOMO energy state are as important as molecular docking results. For example, if we want to predict the inhibitory activity of a new derivative containing a bulkier substituent like ethyl group at position 4, besides obtaining the inhibitory constant

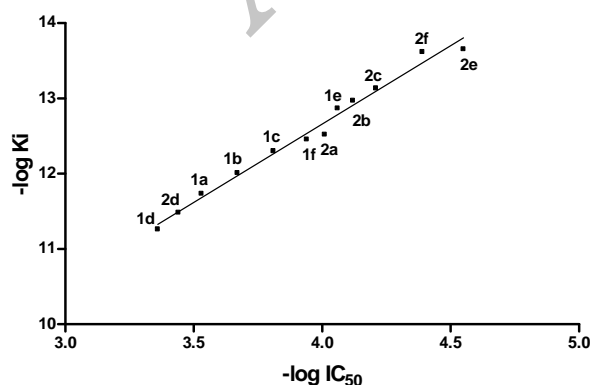


Figure 5. Diagram of ( $-\log K_i$ ) versus ( $-\log IC_{50}$ ) for compounds 1a-f and 2a-f

through docking, we must also determine the difference between the HOMO energy states of this derivative with its 4-H analogs.

## Conclusion

Our molecular modeling studies shows that by using more flexible amino acids during the docking process, more rational results can be obtained. The method of measuring the lipoxygenase activity is also of prime importance for the study of structure activity relationship. The reason behind this argument is based on a comparison that we can make between the results of our previous and present investigations. In our previous study, the enzyme activity was measured by considering the formation of the diene at 234 nm, while we based our recent study on measuring the amount of the peroxide formed at 598 nm. In the previous method, due to the slight solubility of some derivatives and turbidity of their solutions, the error was marginally high in the range of UV wavelength, which had a negative effect on the results of enzyme activity. Furthermore, in the docking investigation, we found that amino acids in the active site of the enzyme were not flexible which reduce the chance of finding a suitable binding space for the inhibitor. Because of these two problems, in our previous investigation we did not get a suitable linear relationship between the results of molecular docking and of enzyme activity. We believe our recent investigation is more comprehensive than our previously reported study.

## Acknowledgment

We are grateful to Mashhad University of Medical Sciences for financial support of this work.

## References

1. Brash AR. Lipoxygenases: Occurrence, functions, catalysis, and acquisition of substrate. *J Biol Chem* 1999; 274:23679-23682.
2. Kuhn H, Thiele BJ. The diversity of the lipoxygenase family. Many sequence data but little information on biological significance. *FEBS Lett* 1999; 449:7-11.
3. Larsen JS, Acosta EP. Leukotriene-receptor antagonists and 5-lipoxygenase inhibitors in asthma. *Ann Pharmacother* 1993; 27:898-903.
4. Schewe T. 15-Lipoxygenase-1: a prooxidant enzyme. *Biol Chem* 2002; 383:365-374.
5. Kelavkar U, Glasgow W, Eling TE. The effect of 15-lipoxygenase-1 expression on cancer cells. *Curr Urol Rep* 2002; 3:207-214.
6. Kelavkar UP, Cohen C, Kamitani H, Eling TE, Badr KF. Concordant induction of 15-lipoxygenase-1 and mutant p53 expression in human prostate adenocarcinoma: correlation with Gleason staging. *Carcinogenesis* 2000; 21:1777-1787.
7. Zhu J, Kilty I, Granger H, Gamble E, Qiu YS, Hattotuwa K, *et al*. Gene expression and immunolocalization of 15-lipoxygenase isozymes in the

- airway mucosa of smokers with chronic bronchitis. *Am J Respir Cell Mol Biol* 2002; 27:666-677.
8. Zhao L, Funk CD. Lipoxygenase pathways in atherogenesis. *Trends Cardiovasc Med* 2004; 14:191-195.
9. Cyrus T, Witztum JL, Rader DJ, Tangirala R, Fazio S, Linton MF, *et al.* Funk CD. Disruption of the 12/15-Lipoxygenase gene diminishes atherosclerosis in Apo E-deficient mice. *J Clin Invest* 1999; 103:1597-1604.
10. Harats D, Shaish A, George J, Mulkins M, Kurihara H, Levkovitz H, *et al.* Overexpression of 15-Lipoxygenase in vascular endothelium accelerates early atherosclerosis in LDL receptor-deficient mice. *Arterioscler Thromb Vasc Biol* 2002; 20:2100-2105.
11. Sultana C, Shen Y, Rattan V. Lipoxygenase metabolites induced expression of adhesion molecules and transendothelial migration of monocyte-like HL-60 cells is linked to protein kinase C activation. *Cell Phys* 1996; 167:477-487.
12. Setty BN, Werner MH, Annun YA, Stuart MJ. 15-hydroxyeicosatetraenoic acid-mediated potentiation of thrombin-induced platelet functions occurs via enhanced production of phosphoinositide-derived second messengers 1,2-diacylglycerol and inositol-1,4,5-trisphosphate. *Blood* 1992; 80:2765-2773.
13. Charlier C, Michaux C. Dual inhibition of cyclooxygenase-2 (COX-2) and 5-Lipoxygenase (5-LOX) as a new start to provide safer non-steroidal anti-inflammatory drugs. *Eur J Med Chem* 2003; 38:645-659.
14. Bakavoli M, Nikpour M, Rahimizadeh M, Saberi MR, Sadeghian H. Design and synthesis of pyrimido[4,5-e][1,3,4] thiadiazine derivatives as potent 15-Lipoxygenase inhibitors. *Bioorg Med Chem* 2007; 15:2120-2126.
15. Bakavoli M, Sadeghian H, Tabatabaei Z, Rahimizadeh M, Nikpour M. SAR comparative studies on pyrimido[4,5-b][1,4]benzothiazine derivatives as 15-Lipoxygenase inhibitors using *ab initio* calculations. *J Mol Model* 2008; 14:471-476.
16. Jabbari A, Davoodnejad M, Alimardani M, Assadieskandar A, Sadeghian A, Safdari H, *et al.* Synthesis and SAR Studies of 3-Allyl-4-prenyloxylaniline Amides as Potent 15-Lipoxygenase Inhibitors. *Bioorg Med Chem* 2012; 20:5518-5526.
17. Caballero J, Fernandez M, Coll D. Quantitative structure-activity relationship of organosulphur compounds as soybean 15-lipoxygenase inhibitors using CoMFA and CoMSIA. *Chem Biol Drug Des* 2010; 76:511-517.
18. Sadeghian H, Seyedi SM, Saberi MR, Arghiani Z. Design and synthesis of eugenol derivatives, as potent 15-Lipoxygenase inhibitors. *Bioorg Med Chem* 2008; 16:890-901.
19. Sadeghian H, Attaran N, Jafari Z, Saberi MR, Pordel M, Riazi M. Design and synthesis of 4-methoxyphenylacetic acid esters as 15-lipoxygenase inhibitors and SAR comparative studies of them. *Bioorg Med Chem* 2009; 17:2327-2335.
20. ChemDraw® Ultra, Chemical Structure Drawing Standard, Cambridge Soft Corporation, 100 Cambridge Park Drive, Cambridge, MA 02140 USA. Available at: <http://www.Cambridgesoft.com>
21. HyperChem® Release 7, Hypercube Inc. Available at: <http://www.hyper.com/>
22. Auto Dock Tools (ADT), the Scripps Research Institute, 10550 North Torrey Pines Road, La Jolla, CA 92037-1000, USA. Available at: <http://www.scripps.edu/pub/olson-web/doc/autodock/>.
23. Morris GM, Goodsell DS, Halliday RS, Huey R, Hart WE, Belew RK, *et al.* Automated Docking using a Lamarckian Genetic Algorithm and an Empirical binding free energy function. *J Comput Chem* 1998; 19:1639-1662.
24. Sippl WJ. Receptor-based 3D QSAR analysis of estrogen receptor ligands-merging the accuracy of receptor-based alignments with the computational efficiency of ligand-based methods. *J Comput Aided Mol Des* 2000; 14:559-572.
25. Iranshahi M, Jabbari A, Orafaie A, Mehri R, Zeraatkar S, Ahmadi T, Alimardani M, Sadeghian H. Synthesis and SAR studies of mono O-prenylated coumarins as potent 15-lipoxygenase inhibitors. *Eur J Med Chem* 2012; 57:134-142.
26. Huey R, Morris GM. Auto Dock Tools; A Tutorial, 2006, 10550 North Torrey pines Road, CA92037-1000, USA.
27. <http://www.accelrys.com/products/discovery-studio>